

Innovative Mechanical Characterization Of Materials By Combining ESPI and Numerical Modelling

C. Barile, C. Casavola, G. Pappalettera, and C. Pappalettere

Abstract—Mechanical characterization of materials allows measuring elastic constants (i.e. Young's modulus, Poisson's ratio, etc.). A complete experimental plan consists of several mechanical tests which may results expensive both in terms of time and costs. Particularly when manufacturing process itself is expensive or when controlling all parameters involved in the manufacturing process is complicated, only a limited number of specimens will be tested and so results risk to be unreliable. The procedure proposed in this work aims to simplify the traditional mechanical characterization of all materials and to obtain the elastic properties by carrying out a reduced number of non-destructive tests.

This new methodology combines two techniques: Electronic Speckle Pattern Interferometry (ESPI) with Finite Element Model (FEM). It works iteratively and proposes to minimize the difference between the displacement fields, experimentally evaluated by ESPI in three-point-bending tests, and their counterpart computed by FEM analysis, applying the same loads and boundary conditions. In this way the approach could be defined as a *hybrid procedure* based on a combination of an optical interferometric technique, commonly used in experimental mechanics, having sub-micrometric sensitivity with a numerical procedure, which uses an optimization algorithm.

Once the procedure has been validated on materials whose properties are known, the purpose of the paper is to accurately evaluate mechanical properties of new materials, today widely applied in numerous fields ranging from aerospace to biomedicine, allowing to deeply reduce experimentation time and costs.

Keywords—Electronic Speckle Pattern Interferometry, FEM analysis, Inverse Problems, Mechanical characterization

I. INTRODUCTION

ONE of the most important phases in mechanical design of components consists in choosing the proper material for a specific application. A good choice should guarantee safety, high mechanical performances and low costs. Designing becomes complex when a new material is chosen. In that case it is necessary to fully characterize the material from a mechanical, physical and chemical point of view. Furthermore it may happen that standards cannot be applied

on these materials and traditional equipment could not be suitable. The traditional approach to mechanically characterize materials is to perform wide experimental campaigns of destructive mechanical tests. Purpose of this study is to well define a new methodology able to significantly reduce the number of tests and the costs experimentation, but ensuring high level of results reliability.

The technique proposed in this paper could be named *hybrid procedure*, as it is based on cooperation of static loading experiments, optimization methods, full-field measurement techniques and a numerical finite element model. This *hybrid procedure* belongs to the big class of the so-called Mixed Numerical–Experimental Technique (MNET) [1], more precisely the one used in this paper fits to the category of inverse problems. In fact, in contrast to a direct problem which is the classical problem where a specified experiment is simulated in order to obtain the stresses and the strains, inverse problems are concerned with the determination of the unknown state of a mechanical system considered as a black box, using information collected from the response to stimuli on the system [2]. It is known that the displacement field of a specimen generally loaded and constrained is univocally defined, through direct measurements only if material properties are known, but when they are unknown or when boundary effects, sample size additions and difficulties in obtaining homogeneous stress and strain fields occur, problem becomes more complex. The inverse problem solution is based on data coming from direct experimental measurements compared with numerical FE-simulation of the same problem. Not only boundary information are used, but relevant data coming from local or full-field surface measurements are also integrated in the evaluation of the behaviour of a given material [3]. As a result of this, in the last years indirect methods using mainly a field information have received increasing attention. One such indirect method is based on measurements of the structure response and application of the numerical-experimental identification technique. The advantage of this inverse method is that non-standardized specimen geometries as well as detailed boundary conditions and complex material models can be taken into account.

Identifying material properties from the indirectly related data sets is referred to as the material reconstruction inverse problem, which has many other applications. For example, in

C. Barile, is with Politecnico di Bari, Dipartimento di Meccanica, Matematica e Management, Bari, 70126 ITALY (corresponding author to provide phone: [+39 0805962812](tel:+390805962812); fax: [+39 0805962777](tel:+390805962777); e-mail: claudia.barile@poliba.it).

C. Casavola, G. Pappalettera, C. Pappalettere, are with Politecnico di Bari, Dipartimento di Meccanica, Matematica e Management, Bari, 70126 ITALY (e-mail: katia.casavola@poliba.it, giovanni.pappalettera@poliba.it, carmine.pappalettere@poliba.it).

structural engineering it is used for structural damage identification [4] and for the characterization of composite materials [5]. It has also been used in robotics design [6], wafer engineering [7], material mechanics [8] and fracture mechanics [9] as well as in biomedical and life science [10]. The application of these methods has no limits as regards the kind of material to be tested nor as regards the experimental set-up to be used. It has been applied on materials like composite for identifying the four independent elastic in-plane engineering constants [3], ceramics to evaluate elastic properties [11], wood for viscoelastic characterization [12] and metals [13]. Moreover numerous attempts have been made to identify elastic parameters based on inverse modelling of different experimental set-ups. Some researchers use uniaxial open hole tensile tests [14], or plane biaxial tensile tests on cruciform specimens or on a holed plate [3, 15], others use a circular disk under diametrical compression [16] or a T-shaped specimen under tensile loading [17]. From an experimental point of view, the progress made during the last decade in the domain of optical full-field displacement techniques now allows the experimental identification of complex strain fields. Scientific literature is rich of applications of different optical full-field techniques for the measurement of the surface displacements [18]: laser holographic interferometry [19], ESPI [20-23] and geometric or interferometric moiré [24]. In some cases researchers combine experimental tests with the virtual fields method [25] or with the boundary element method (BEM) [26] instead of the finite element analysis [27], but the general principle of such *hybrid procedure* remains identical.

For this reason it appears that an efficient material characterization procedure should determine all the elastic constants by performing a very limited number of experimental tests. Hybrid techniques, which minimize the difference between experimental and numerical data using optimization algorithms where elastic constants are included as design variables, certainly satisfy such a requirement and are actually increasing their application in practical engineering. It is obvious that a suitable hybrid technique will need: a simple experimental setup able of precise and non-invasive full field measurements, a robust and reliable optimization procedure capable to converge to the target values of elastic properties independently of the load type, initial guess on elastic constants, boundary conditions, etc. [27].

In this paper the *hybrid procedure* described combines the phase-shifting Electronic Speckle Pattern Interferometry with Finite Element Modelling, in order to evaluate elastic properties (Young's modulus E , Poisson's ratio ν) of metals, sintered, composites materials and woods by an inverse solution of the elastic problem.

For our purpose ESPI [28, 29] is preferred in view of its capability to accurately measure displacements in real time and to gather full field information without altering specimen conditions. ESPI can, in principle, measure displacement components $u(x, y, z)$, $v(x, y, z)$ and $w(x, y, z)$ for each point (x, y, z) of the specimen surface. When the real-time speckle

pattern is subtracted from a reference one, a system of fringes will appear on the specimen surface and each fringe represents the locus of an iso-displacement region along the sensitivity direction defined by the geometry of the set-up. The frequency distribution of fringes can be used for recovering strain fields. This full-field optical technique is used to evaluate the displacement field of specimens made of different materials subjected to three-point-bending experimental tests. The experimental protocol is chosen in order to avoid rigid body motion and prevent speckle pattern decorrelation: for this reason the horizontal displacement component is monitored instead of the greater vertical one; moreover it is sufficient to apply a low level of load to the specimen and this simplify the loading system. At the same time an innovative algorithm, implemented in a numerical model, automatically executes several optimization loops varying E and ν in order to minimize the objective function based on the difference between displacements evaluated by means of ESPI and the same predicted by FEM analysis. Conversely to other analytical approach this numerical model has no need of complex or variable geometry to get convergence, it only requires a simple plate with rectangular cross section having any dimensions. The shape of the specimen doesn't influence the numerical analysis as it happens for virtual field methods [25].

The methodology is firstly applied on material whose properties are known, as titanium, in order to define the set-up and to test its reliability by evaluating the quality of the measurements. Then it is applied on different materials: sintered by means of Selective Laser Melting technique (SLM) and orthotropic wood's laminate.

II. MATERIALS AND METHODS

The prospect of using this approach on all kind of materials depends on the level of reliability that it reaches if used to characterize a traditional material as grade 5 titanium (Ti6Al4V) [30]. Once validated it was applied on Selective Laser Melting (SLM) parts and on wood specimens due to the fact that they have great interest in engineering field and also because they are difficult to be accurately characterized by traditional approaches.

In SLM technique parts were built by adding layers of metal powder. A focused laser beam is used to fuse the powder material by scanning cross-sections generated from a 3D CAD model of the part on the surface of the powder bed. After each cross-section is scanned a new layer of material is applied on top, the powder bed is lowered by one layer thickness and the process is repeated until the part is completed. In order to obtain high density parts the powder mixture and SLM process parameters must be optimized, but this manufacturing process modifies the initial mechanical characteristics of metal powders, which strongly depend on process parameters (i.e. laser energy, scanning strategy, etc.) and are hardly predictable. Since controlling all parameters involved in the manufacturing process may be very complicated, accurate mechanical characterization of SLM components was mandatory to properly assess mechanical response. Building

SLM parts was rather expensive, so traditional mechanical tensile tests are generally executed on a limited number of specimens that not ensure a fully mechanical characterization. The hybrid procedure proposed in this work represents a good solution to solve this problem overcoming all the limitations described.

Engineered wood products, glued building products engineered for application-specific performance requirements, are often used in construction and industrial applications. Glued engineered wood products are manufactured by bonding together wood strands, veneers, lumber or other forms of wood fibres with glue to form a larger, more efficient composite structural unit. Engineered wood products prove to be more environmentally friendly and, if used appropriately, are often less expensive than building materials such as steel or concrete. These products are extremely resource-efficient because they require fewer resources and produce minimal waste.

Wood is a hard, fibrous tissue. It has been used for many years for both fuel and as a construction material. It is an organic material, a natural composite of cellulose fibres (which are strong in tension) embedded in a matrix of lignin, which resists compression. Wood may also refer to other plant materials with comparable properties, and to material engineered from wood, or wood chips or fibre. There is a strong relationship between the properties of wood and the properties of the particular tree that yielded it. The density of wood varies with species and it is correlates with its strength (mechanical properties).

For our purpose plywood specimens were tested. Plywood is a heterogeneous, hygroscopic, cellular and anisotropic material. It is composed of cells, and the cell walls are composed of micro-fibrils of cellulose and hemicellulose impregnated with lignin. Since wood has different behaviour in relation with the percentage of fibres, fibre direction and presence of imperfections (e.g. knot), this material results expensive and difficult to characterize by using traditional tests [31].

III. EXPERIMENTAL TESTS

A three-point bending test was carried out on specimens, having plate geometry. Specimens were placed on two supports placed at a distance of 90 mm. The loading apparatus, shown in Figure 1, consists of a 2 kg loading cell DS514QD connected to the wedge that measure the applied load. The load was transferred by a micrometric translation stage which pushes the loading wedge against the specimen.

Instead of the strain gauges, ESPI was chosen to monitor the displacement field of the specimen. It is a powerful full-field optical technique able to provide high accuracy results with non-contact requirements and to avoid the errors associated with the strain gauges application. The technique is based on the fact that two beams originated from a coherent light source (i.e. laser) produce an interferometric pattern from which we can recover either correlation fringes and/or phase distribution. Correlation fringes and/or phase distribution are utilized to compute displacements, which are proportional to

correlation fringe order or to phase difference between loaded and reference (i.e. unloaded) state. As it is known, phase-stepping strategies in speckle interferometry are very useful since they allow us to recover directly the phase value at each point of the specimen surface. N different interferometric patterns are taken at two different exposures: the reference (i.e. unloaded) and the loaded one. From each set of N acquisition, it is possible to get the distribution of phase $\phi(x, y)$ at each point of the surface. Finally, displacement are easily computed as they are proportional to the $\Delta\phi(x, y)$ difference between two exposures.



1. Micrometric translation stage
2. Loading wedge
3. Supporting wedges
4. Mirror
5. PZT translation stage

Fig. 1 Loading apparatus and detail of the optical setup

Samples were preloaded in order to minimize rigid body motions, which may cause speckle decorrelation. In any case very low values of displacement were induced on the specimens and the horizontal displacement component was monitored instead to the greater vertical one. The preload was centred on the upper surface sample. Depending on the type of material, a thin coating layer was sprayed onto the specimen surface to improve contrast of speckle fringes. The scheme of the optical set-up used for measuring u-displacements is shown in Figure 2.

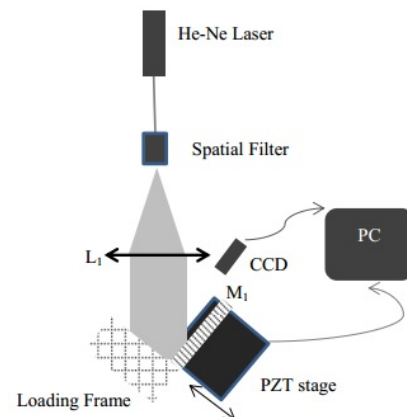


Fig. 2 Schematic of the double illumination ESPI setup

In order to ensure a correct application of the load, 4 strain gages were placed on the specimens' surface: 2 on the upper surface along the axis and far 10 mm from the edges, 2 on the lower surface in correspondence of the middle section and far 5 mm from the lateral edges (Figure 3). The real values obtain from the strain gages during the test, confirm that the load was uniformly distributed and was exactly applied in the middle section of the specimen.

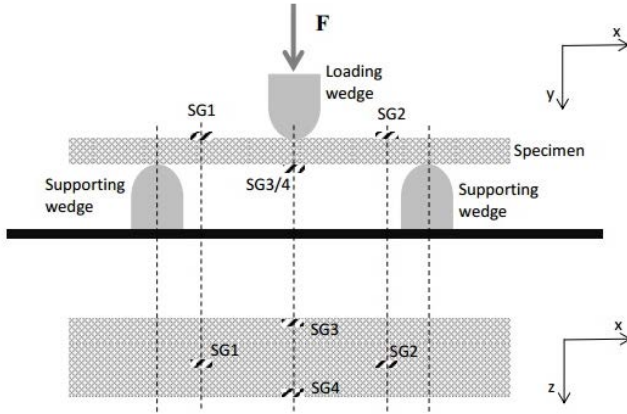


Fig. 3 Scheme of strain gauges application

Set-up essentially consists of a double illumination Lendeertz interferometer [29]. The light emitted by a 17 mW He-Ne laser source ($\lambda = 632.8$ nm) is expanded by a 20X microscope objective lens and spatially filtered by a 10 μm aperture pin-hole. The beam emerging from the pin-hole is successively collimated by the L1 plano-convex lens ($\phi = 2$ inch, $f = 40$ cm). One half of the beam is then sent towards the specimen under testing at the illumination angle $\theta_1 = 45^\circ$. The rest of the beam is intercepted by the planar mirror M1 that reflects the light towards the specimen thus realizing symmetric double illumination. The mirror is placed on a piezoelectric translation stage (PZT), which allows the motion along the horizontal direction, parallel to the direction of sensitivity. The PZT is driven by a stabilized high-voltage power supply controlled by a personal computer. The minimum incremental displacement that can be generated is $d_m = 10$ nm. Each beam generates a speckle pattern on the specimen surface. The superposition of those patterns leads to have the following distribution of intensity:

$$I(x, y) = I_{01}(x, y) + I_{02}(x, y) + 2\sqrt{I_{01}(x, y)I_{02}(x, y)} \cos[\gamma(x, y)] \quad (1)$$

where I_{01} and I_{02} are the reference and object intensities while γ is the phase difference between the beams. If a point of the specimen surface displaces along the direction of sensitivity, the equation (1) can be rewritten as:

$$I(x, y) = I_{01}(x, y) + I_{02}(x, y) + 2\sqrt{I_{01}(x, y)I_{02}(x, y)} \cos[\gamma(x, y) + \Delta\phi(x, y)] \quad (2)$$

The phase difference $\Delta\phi$ is related to the u-displacement by the following equation:

$$\Delta\phi = \frac{4\pi}{\lambda} u \sin \theta \quad (3)$$

Fringes are hence iso-displacement *loci* and the difference in displacement between points lying on two adjacent fringes is:

$$u = \frac{\lambda}{2 \sin \theta} n_x \quad (4)$$

where n_x represents the fringe order.

According to equation (4), the sensitivity of the adopted optical set-up is 447 nm.

Phase shifting was utilized in order to obtain the phase distribution of the speckle pattern. To that purpose, a shift in phase between the two beams was introduced by changing the optical path of one of the arms of the interferometer. Phase variations were produced by moving the PZT stage. Among the different phase shifting strategies available in literature [28, 32], the five frame algorithm which consists in recording five interferograms with a relative phase shift $\delta = \frac{\pi}{2}$ was utilized (Figure 4).

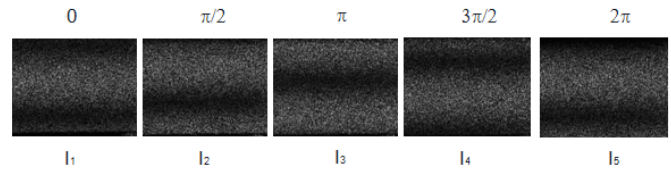


Fig. 4. Recorded images of five frame technique

The intensity patterns corresponding to each phase shift can be described by the following equation:

$$I_n(x, y) = I_{01}(x, y) + I_{02}(x, y) + 2\sqrt{I_{01}(x, y)I_{02}(x, y)} \cos\left[\gamma(x, y) + \Delta\phi(x, y) + n\frac{\pi}{2}\right] \quad (5)$$

Finally, the phase difference is computed as follows:

$$\Delta\phi = \arctan \frac{2[I_1(x, y) - I_4(x, y)]}{2I_3(x, y) - I_5(x, y) - I_1(x, y)} \quad (6)$$

The PZT was calibrated by recording an initial speckle pattern and moving the mirror at incremental steps of 10 nm. The speckle pattern corresponding to each shifted position was subtracted from the initial speckle pattern until a minimum of intensity was observed. The corresponding distance travelled by the PZT was related to the change of optical path yielding a 2π phase shift. Calibration of the camera pixel was done by recording the image of a calibration target and sampling the distance between two calibration marks with a certain number of pixels. The spatial calibration was 15 μm . In the processing phase for each shift of phase the difference between the recorded image and the reference image was

determined by digitally subtracting speckle patterns. A 7×7 pixel square median filter was then applied to the five images in order to reduce noise. A mask was applied in order to select the region of interest. Equation (6) was used in order to obtain the wrapped phase. Phase unwrapping operation was carried out by means of the minimum spanning tree algorithm [33]. Finally, displacement maps were recovered by using the scaling equation (4).

IV. NUMERICAL MODEL

The values of the material parameters cannot be derived immediately from the experiment. A numerical analysis is necessary to simulate the actual experiment. However, this requires that the material parameters are known. The identification problem can then be formulated as an optimization problem where the function to be minimized is some error function that expresses the difference between numerical simulation results and experimental data [3]. In the present case the displacements are used as output data. Figure 5 represents the flow-chart of the present inverse modelling problem. The parameters to be identified are the two independent engineering constants E and ν .

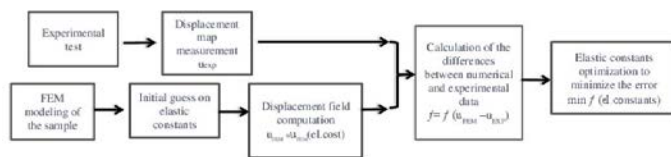


Fig. 5. Flow chart of hybrid procedure

A finite element model was developed in order to reproduce the three-point-bending experiments and simulate the mechanical behaviour of all materials tested. Sizes, geometry, loads and constraints were modelled in respect of the real conditions.

Because of structural symmetry, only one half was modelled. Kinematic constraints were imposed in order to obtain a symmetric model and to correctly reproduce the mechanism of loading. The region of interest considered along the x -direction was about 63 mm, the same area was used in the numerical model to measure u -displacement and to compare results. The area monitored during experimental test

was located 500 nm far from the constraint wedge and far enough from the region where the load was applied, in order to avoid the influence of local phenomena. Attempt values of Young's modulus and Poisson's ratio were inserted in the simulation.

The optimization process get involved in the model varying the elastic constants until the difference between numerical and experimental displacements was minimized. For any specimen to be characterized and which has been subjected to some loading condition, it is possible to express the difference between experimental data and analytical/numerical predictions by means of an error function W , which depends on the elastic constants of the material. The W error will decrease as the elastic constants come close to their target values. Here, we build the W function as the difference between the displacement field measured with speckle interferometry and its counterpart computed by means of finite element analysis [27].

FE analysis was carried out with the ANSYS® commercial software [34]. The specimen was modelled with three-dimensional solid elements including 8 nodes each of which has 3 degrees of freedom. Although the thickness of the specimens is small compared to length, the specimen under three-point-bending was modelled as a 3D specimen in order to account for asymmetries eventually occurring in the loading process or related with constraint conditions.

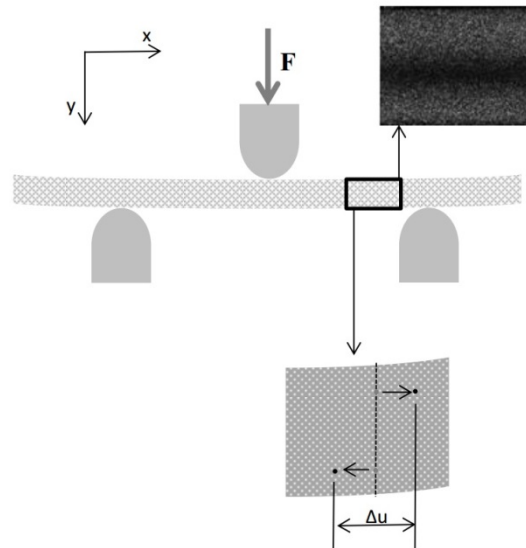


Fig. 6. The region of interest compared between experimental and numerical analysis

Convergence analysis was carried out in order to refine the model and to obtain a mesh independent solution. Mesh size was consistent with sampling of the speckle pattern. The mesh typically included about 50000 elements and 60000 nodes. Figure 6 with indications of loads and constraints is representative of all materials.

The optimization method used to evaluate the unknown elastic constants of materials, for this hybrid procedure, was the first order method. The first order method was based on design sensitivities and was more suitable for problems that require high accuracy. The program performed a series of analysis-evaluation-modification cycles. An analysis of the

initial design was performed, the results were evaluated against specified design criteria, for our purpose the minimization of difference between experimental and numerical displacements, and the design was modified as necessary. The process was repeated until all specified criteria were met. The first order method converted the problem to an unconstrained one by adding penalty functions to the objective function. However the actual finite element representation was minimized and not approximated.

The first order method used gradients of the dependent variables with respect to the design variables. For each iteration, gradient calculations (which may employ a steepest descent or conjugate direction method) were performed in order to determine a search direction, and a line search strategy was adopted to minimize the unconstrained problem. Each iteration was composed of a number of sub iterations that included search direction and gradient computations. That is why one optimization iteration for the first order method performed several analysis loops.

First order iterations continued until either convergence was achieved or termination occurs. The problem was said to be converged if, when comparing the current iteration design set to the previous and best sets, one of the following conditions was satisfied:

- the change in objective function from the best design to the current design was less than the objective function tolerance

$$W_{\text{current}} - W_{\text{optimum}} < W(\text{Tolerance})$$

- the change in objective function from the previous design to the current design was less than the objective function tolerance

$$W_{\text{current}} - W_{\text{previous}} < W(\text{Tolerance})$$

It was also a requirement that the final iteration used a steepest descent search, otherwise additional iterations were performed. Young's modulus and Poisson's ratio became the design variables and the vector design variables was defined as:

$$x = [E, \nu]$$

Also the design constraints were imposed:

$$\begin{cases} \underline{E}_i < E < \overline{E}_i \\ \underline{\nu}_i < \nu < \overline{\nu}_i \end{cases}$$

where

- ($i=1,2,3,\dots,n$)
- \underline{E}_i and \overline{E}_i were respectively the lower and upper Young's modulus limits
- $\underline{\nu}_i$ and $\overline{\nu}_i$ were respectively the lower and the upper Poisson's ratio limits.

Initial values of elastic constants E and ν were assumed. Since the comparison with the experimental values was related to u-displacement field, along the x-axis, the objective function was defined as:

$$W = \left| \frac{[U_{\text{Node}}(\text{Trax}) - U_{\text{Node}}(\text{Comp})]_{\text{FEM}} - U_{\text{EXP}}}{U_{\text{EXP}}} \right| \quad (7)$$

where $U_{\text{Node}} = f(x)$ and $U_{\text{EXP}} = f(x)$, $U_{\text{Node}}(\text{Trax})$ represents the maximum value of displacement in correspondence of stretched fibers, $U_{\text{Node}}(\text{Comp})$ is the minimum value of displacement in correspondence of compressed fibers and U_{EXP} represents the delta value of displacement measured experimentally between stretched and compressed fibres. All these values were chosen for a given specimen section. As results Equation (7) represents the difference of displacements between experimental and numerical results.

V. RESULTS AND ANALYSIS

The horizontal displacement measured by ESPI was taken as target value of FE analysis. In all materials tested (grade 5 titanium, SLM parts and wood specimens), as it was said, the area monitored during experimental test was located 500 nm far from the constraint wedge and far enough from the region where the load is applied, in order to avoid the influence of local phenomena. Following results of all materials tested are presented. They show firstly titanium specimens, since it is used to define the experimental set up and to validate the approach that could be used to study all kind of materials. Once the reliability of the approach is confirmed then the same methodology is applied on sintered and wood specimens.

Titanium is an isotropic material. Samples were subjected neither to thermal treatment either to mechanical process that could modify the material properties. Young's modulus of Ti6Al4V, used as target values for design variables in the numerical model, was 110 GPa [35] while Poisson's ratio was fixed to 0.32. On the other hand starting values were respectively $E=180$ GPa and $\nu=0.30$. The optimization algorithm minimizes the gap between displacement measured by ESPI (Δu_x , Exp) and those evaluated by FEM analysis (Δu_x , FEM). Table 1 summarizes results related to the optimization process: it can be observed that the error on measured displacements decreases as the loading level increases and also that the residual error on displacements is less than 1%. Mechanical properties calculated for titanium alloy by means of the proposed hybrid procedure were respectively $E=109$ GPa and $\nu=0.30$. The results obtained were in agreement with the literature ones, so it results that the proposed methodology works well [20].

Table 1 Optimization results for titanium

Load [g]	Δu_x Exp Fit [nm]	Δu_x Exp FEM [nm]	Error [%10 ⁻⁴]	E [GPa]	ν
304	313.45	313.42	6.70	109.00	0.299
467	499.05	499.05	4.62	110.23	0.299
690	729.07	729.06	3.80	109.01	0.299
870	957.95	957.95	0.17	109.90	0.299
1072	1187.97	1187.96	0.64	109.20	0.298

Fig. 7 summarizes the convergence procedure on titanium specimen for one loading step, in order to validate the algorithm function used in the optimization procedure.

Difference between experimental and numerical results decreases increasing the iterations number.

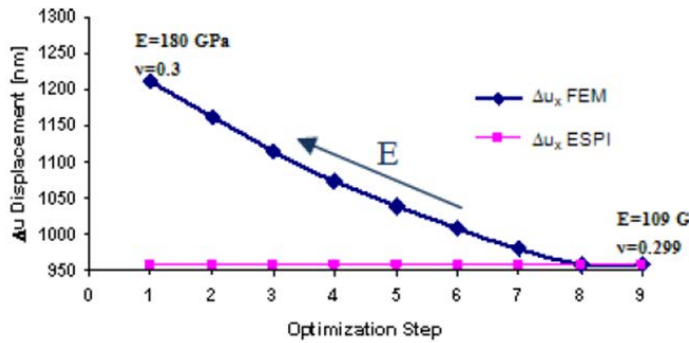
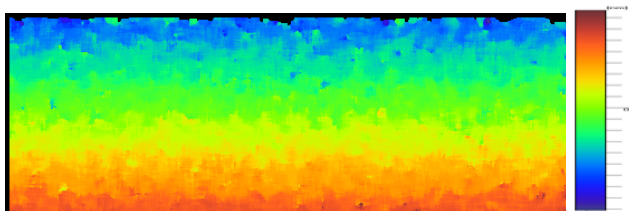


Fig. 4 Titanium optimization trend

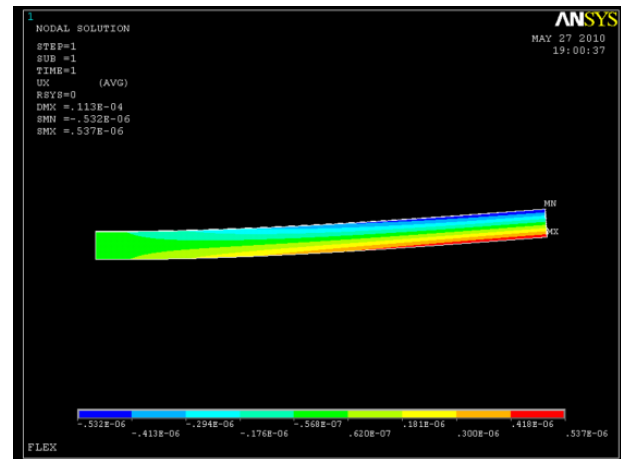
Sintered material was assumed as isotropic and linearly elastic. This modelling choice was justified by the fact that SLM specimens were realized layer by layer and each layer may be considered as isotropic. The experimental evidence seems to confirm this assumption: in fact, the u_x displacement measured through the thickness became null at the specimen midplane. Mechanical characterization of SLM starts from Young’s modulus of 166 GPa related with specimens built with very similar process parameters, as the SLM parts studied in this work, tested in previous papers [36].

The calculation procedure was lead in different steps. At the beginning only Young’s modulus was optimized, then also Poisson’s ratio was introduced. Moreover the loading steps were increased, in order to obtain a large number of terms of comparison between experimental tests and numerical models.

As expected iso u -displacement bands are almost parallel in the specimen near the supporting wedges. The experimental pattern (Figure 8 a) is in excellent agreement with FE results (Figure 8 b). The difference in displacement between points located on vertical lines at different distances from the constrained edge of the specimen was found to be insensitive to the position. The same conclusion can be drawn for all load levels considered in the experiments.



(a)



(b)

Fig. 8 (a) Horizontal displacement map near supporting wedge of the sintered material; (b) Horizontal displacement map evaluated via FEM of the sintered material

Remarkably, the experimentally measured values of u -displacement were found to be symmetric with respect to the neutral midplane of the specimen. This seems to confirm the assumption of isotropy of SLM material made in the numerical analysis. Table 2 shows the results obtained by perturbing elastic constants. Also in this case the proposed methodology seems to work: the error on measured displacements decreases as the loading level increases and also that the residual error on displacements is less than 1%. Mechanical properties calculated for SLM specimen are: Young’s modulus=132 GPa and Poisson’s ratio= 0.30. It results important that the weight of Poisson ratio in FEM optimization is absolutely lower than the Young modulus, probably because the material was treated as an isotropic one [21, 22, 37].

Table 2 Optimization results for SLM

Load [g]	Δu_x Exp Fit [nm]	Δu_x FEM [nm]	Error [%E-05]	E [GPa]	ν
293	489.78	489.780	2.500	131.33	0.299
330	550.73	550.729	0.290	131.54	0.299
504	837.34	837.340	0.026	132.13	0.299
529	878.52	878.520	0.015	132.19	0.299
695	1151.95	1151.950	0.052	132.45	0.299
706	1170.07	1170.069	0.220	132.46	0.299
810	1341.38	1341.382	0.120	132.56	0.299

In order to verify the validity of hybrid procedure for orthotropic material another material was tested. For our purpose it was considered a plywood specimen, composed of five layers having two different thicknesses according to the orientation of the fibres.

It should be noted that the common practice of testing material involves the use of strain gauges. But ensuring a correct application of these transducers implies:

1. the choice of a proper adhesive for porous material in order to avoid the reinforcement effect

2. the gage bonding on a proper position to ensure the reading of strains for all the laminate and not only for a single lamina
3. the choice of the correct pressure grips to ensure a total tightening but not to compromise the integrity of the component (e.g. tensile test in order to obtain the elastic properties).

For these reasons an uniaxial flexural test was applied and an optical technique was used to evaluate the field displacements. The first approach of this study concerned with the macroscopic identification of the mechanical properties of the wood [38]. Five plies constituted the laminate:

- 2 plies with fibres parallel to the longitudinal axes of specimen; each ply was 2.5 mm thick
- 3 plies with fibres perpendicular to the longitudinal axes of specimen; each ply was 1.03 mm thick (Figure 9).

In the finite element analysis the specimen was modelled as a single isotropic block of wood. In fact it was supposed that the target value of the elastic modulus was the weighted average of the longitudinal and the transverse elastic moduli related to the thickness of each ply and the percentage of fibres'. The values of these elastic properties reported in literature were [38-40]:

- $E_L \approx 10$ GPa
- $E_T \approx 0.4$ GPa
- $\nu = 0.3 \div 0.4$

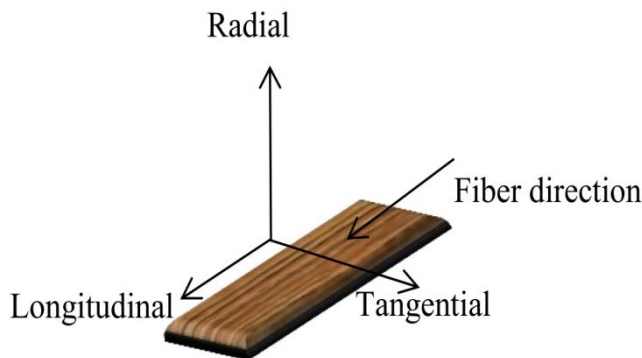


Fig. 9. Schematically reference axes of wood laminate

So the mean target value in the numerical model was calculated considering the weighted thickness referred to orientation of the fibres and the weighted average of E_L and E_T : $E_{\text{mean}}=6.4$ GPa.

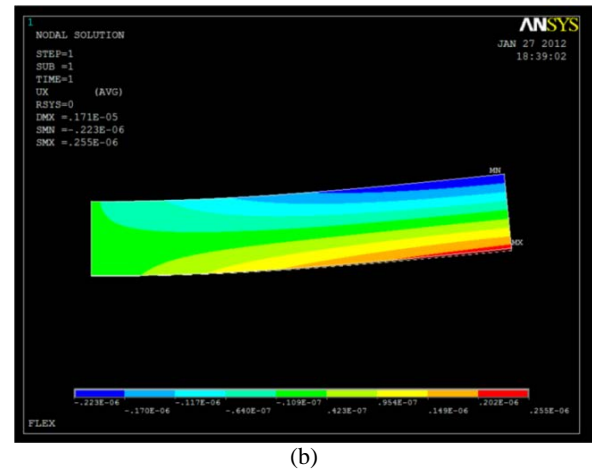
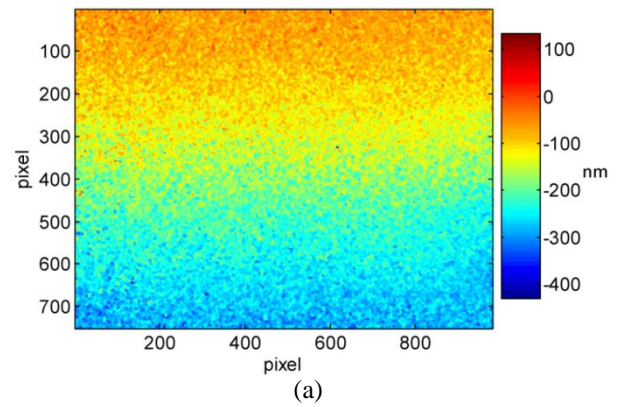


Fig. 10 (a) Experimental displacement map of a plywood specimen subjected to 200g load; (b) FEM displacement map of a plywood specimen subjected to 200g load

As a first approach to mechanically characterize wood, the design variables for the optimization analysis were respectively the mean value of elastic modulus along the specimen longitudinal axis (E) and the Poisson's ratio (ν) representative for a hypothetical isotropic plate. Two load steps were applied on the sample: 100 g and 200 g. Higher loads should be avoided because fringe quality could decrease due to speckle decorrelation. The experimental displacement map relative to a load of 200 g provides a value of Δu_x of about 450 nm (Figure 10 - a).

The FE analysis applied on a model with the same sizes, load and constraints provides a value of about 445 nm (Figure 10 - b), in good agreement with the experimental one. The value of Poisson's ratio correspondent to this value of displacement was 0.3, the value of elastic modulus for this value of displacement is $E=6.4$ GPa consistent with the weighted average of literature values [23]. Also in this case iso u -displacement bands are almost parallel in the specimen region near the supporting wedges for all loading steps.

VI. CONCLUSIONS

The hybrid procedure adopted in this paper proved itself to provide good results in determining mechanical properties on a class of different materials. The numerical results seem to be in good agreement with the experimental ones. Developments in progress are about the complete and precise characterization

of all orthotropic and anisotropic materials in order to provide a fully database of both elastic and plastic properties that can be used in industrial and academic field as support for mechanical characterization.

REFERENCES

- [1] H. Sol, H. Hua, J. De Visscher, J. Vantomme and W.P. De Wilde, "A mixed numerical/experimental technique for the nondestructive identification of the stiffness properties of fibre reinforced composite materials", *NDT-E International*, vol. 30, pp. 85-91, 1997.
- [2] H.D. Bui, "Inverse Problems in the Mechanics of Materials: An Introduction", *CRC Press Inc.*, Florida, 1994.
- [3] D. Lecompte, A. Smits, H. Sol, J. Vantomme, and D. Van Hemelrijck, "Mixed numerical-experimental technique for orthotropic parameter identification using biaxial tensile tests on cruciform specimens", *International Journal of Solids and Structures*, vol. 44, pp. 1643-1656, 2007.
- [4] H.P. Chen, and N. Bicanic, "Inverse damage prediction in structures using nonlinear dynamic perturbation theory", *Computational Mechanics*, vol. 37, no.5, pp. 455-67, 2006.
- [5] E.J. Garboczi, and A.R. Day, "Algorithm for computing the effective linear elastic properties of heterogeneous materials - 3-dimensional results for composites with equal phase Poisson ratios", *Journal of the Mechanics and Physics of Solids*, vol. 43, no. 9, pp. 1349-62, 1995.
- [6] A. Joukhadar, T. Garat, and C. Laugier, "Constraint-based identification of a dynamic model", *In: Proceedings of the intelligent robots systems (IROS'97)*, 1997.
- [7] D.R. Franca, and A. Blouin, "All-optical measurement of in-plane and out-of-plane Young's modulus and Poisson's ratio in silicon wafers by means of vibration modes", *Measurement Science and Technology*, vol. 15, no.5, pp. 859-68, 2004.
- [8] C. A. Brebbia, and A. A. Mammoli, *Computational Methods and Experiments in Materials Characterization II*, WIT Press, 354 pp., 01 gen 2005.
- [9] G. Maier, M. Bocciarelli, G. Bolzon, and R. Fedele, "Inverse analyses in fracture mechanics", *International Journal of Fracture*, vol. 138, no. 1-4, pp. 47-73, 2006.
- [10] L.G. Han, M. Butcher, and J.A. Noble, "Non-invasive measurement of biomechanical properties of in vivo soft tissues", *Medical Image Computing and Computer - Assisted Intervention-Miccai 2488 (Pt 1)*, pp. 208-15, 2002.
- [11] F.M. Furgiuele, M. Muzzupappa, and L. Pagnotta, "A full-field procedure for evaluating the elastic properties of advanced ceramics", *Experimental Mechanics*, vol. 37, pp. 285-291, 1997.
- [12] L. Le Magorou, F. Bos, F. Rouger, "Identification of constitutive laws for wood-based panels by means of an inverse method", *Composites Science and Technology*, vol. 62, pp. 591-596, 2002.
- [13] M. Meuwissen, "An Inverse Method for the Mechanical Characterization of Metals", *Ph.D. Thesis*, Eindhoven University of Technology, The Netherlands, 1998
- [14] J. Molomard, R. Le Riche, A. Vautrin, and J.R. Lee, "Identification of the four orthotropic plate stiffnesses using a single open-hole tensile test", *Experimental Mechanics*, vol. 45, no. 5, pp. 404-411, 2005.
- [15] J.F. Cárdenas-García, S. Ekwaro-Osire, J.M. Berg, and W.H. Wilson, "Non-linear least-squares solution to the Moiré hole method problem in orthotropic materials. Part II: Material elastic constants", *Experimental Mechanics*, vol. 45, no. 4, pp. 314-324, 2005.
- [16] Z. Wang, J.F. Cárdenas-García, B. Han, "Inverse method to determine elastic constants using a circular disk and Moiré interferometry", *Experimental Mechanics*, vol. 45, no. 1, pp. 27-34, 2005.
- [17] M. Grédiac, F. Pierron, and Y. Surrel, "Novel procedure for complete in-plane composite characterization using a single T-shaped specimen", *Experimental Mechanics*, vol. 39, pp. 142-149, 1999.
- [18] O. Zeleniuc, A.M. Varodi, V. Petrovici, and A-M.L. Badescu, "Mechanical properties of wooden laminated structures glued with a furan resin based adhesive", *Proceedings of the International Conference on Urban Sustainability, Cultural Sustainability, Green Development Green Structures and Clean Cars*, pp. 143-147, 2010.
- [19] J. Zhu, "Measurement of Poisson's ratio of non-metallic materials by laser holographic interferometry", *Proceedings of the 14th WCNDT, New Delhi*, India, pp. 1481-1484, 1996.
- [20] C. Barile, C. Casavola, G. Pappaletta, and C. Pappaletta, "Mechanical characterization of orthotropic materials with speckle interferometry and numerical optimization", *Proceedings Youth Symposium on Experimental Solid Mechanics*, Trieste, Italy, (2010).
- [21] C. Barile, C. Casavola, G. Pappaletta, and C. Pappaletta, "Mechanical characterization of SLM specimens with speckle interferometry and numerical optimization", *Conference Proceedings of the Society for Experimental Mechanics Series*, vol. 6, pp. 837-843, 2011.
- [22] C. Barile, C. Casavola, G. Pappaletta, and C. Pappaletta, "Experimental and numerical characterization of sinterized materials with speckle interferometry and optimization methods", *10th IMEKO TC15 Youth Symposium on Experimental Solid Mechanics 2011*, Chemnitz (Germany), 25-28 May 2011.
- [23] C. Barile, C. Casavola, G. Pappaletta, and C. Pappaletta, "Hybrid Characterization of Laminated Wood with ESPI and Optimization Method", *Conference Proceedings of the Society for Experimental Mechanics Series*, vol. 3, pp. 75-83, 2013.
- [24] J.F. Cárdenas-García, "Determination of the elastic constants using Moiré", *Mechanics Research Communications*, vol. 27, no. 1, pp.69-77, 2000.
- [25] M. Grédiac, F. Pierron, "Applying the Virtual Fields Method to the identification of elasto-plastic constitutive parameters", *International Journal of Plasticity*, vol. 22, pp. 602-627, 2006.
- [26] L. Huang, X. Sun, Y. Liu, Z. Cen, "Parameter identification for two-dimensional orthotropic material bodies by the boundary element method", *Engineering Analysis with Boundary Elements*, vol. 28, pp. 209-221, 2004.
- [27] K. Genovese, L. Lamberti, and C. Pappaletta, "A new hybrid technique for in-plane characterization of orthotropic materials", *Experimental Mechanics*, vol. 44, no. 6, pp.584-592, 2004.
- [28] G.L. Cloud, *Optical Methods in Engineering Analysis*, Cambridge University Press, New York USA, 1998.
- [29] C. Sciammarella, "Overview of optical techniques that measure displacements: Murray Lecture", *Experimental Mechanics*, vol. 43, no. 1, pp. 1-19, 2006.
- [30] S. Velicu, D.-A. Coroni, M. Iliescu, "Study on Machinability of Ti6Al-4V Titanium Alloy in Turning", *Advances in Production, Automation and Transportation Systems*, pp. 223-226, 2013.
- [31] L. Pagnotta, and G. Stigliano, "Identification of composite plate elastic properties by displacement field measurement", *Proceedings of the 2nd WSEAS Int. Conference on Applied and Theoretical Mechanics*, Venice, (Italy), 20-22 November, 2006.
- [32] K. Creath, "Phase shifting speckle interferometry", *Applied Optics*, vol. 24, no. 18, pp. 3053-3058, 1995.
- [33] N.H. Ching, D. Rosenfeld, and M. Braun, "Two-dimensional phase unwrapping using a minimum spanning tree algorithm", *IEEE Transactions on Image Processing*, vol. 1, no. 3, pp. 355-365, 1992.
- [34] The ANSYS Users' Manual, Swanson Analysis System Inc., 2013
- [35] C. Casavola, C. Pappaletta, and F. Tattoli, "Experimental and numerical study of static and fatigue properties of titanium alloy welded joints", *Mechanics of Materials*, vol. 41, no. 3, pp. 231-243, 2008.
- [36] C. Casavola, S.L. Campanelli, and C. Pappaletta, "Preliminary investigation on the residual strain distribution due to the Selective Laser Melting Process", *Journal of Strain Analysis*, vol. 44, no. 1, pp. 93-104, 2009.
- [37] C. Barile, C. Casavola, G. Pappaletta, and C. Pappaletta, "Mechanical characterization of SLM specimens with speckle interferometry and numerical optimization", *Society for Experimental Mechanics - SEM Annual Conference and Exposition on Experimental and Applied Mechanics*, vol. 3, pp. 2523-2529, 2010.
- [38] The Engineering Toolbox. The engineering toolbox (2012)
- [39] MatWeb. Matweb material property data (2012)
- [40] D.W. Green, J.E. Winandy, and D.E. Kretschmann, *Wood handbook - Wood as an engineering material*, Forest Products Laboratory, 1999.